PREDATOR-PREY MODEL WITH MONOD-HALDANE FUNCTIONAL RESPONSE AND FEAR EFFECT ON PREY DYNAMICS

Nadila Agustin Eka Wulandari[1], Dian Savitri[1*]

[1] *Department of Mathematics, Faculty of Mathematics and Natural Science, Universitas Negeri Surabaya, Indonesia*

Article Info

Article history:
Received July 23th, 2025
Revised October 5th, 2025
Accepted October 15th, 2025

Corresponding Email:
diansavitri@unesa.ac.id

ABSTRACT

This study investigates a predator–prey model incorporating the Monod–Haldane functional response and the fear effect on prey. The objective of this research is to analyze population dynamics and system stability under the influence of prey fear. The model is examined through equilibrium and stability analysis and verified using numerical simulations with phase portraits. The results demonstrate that the fear effect significantly alters the stability of the interior equilibrium point and affects predator–prey population dynamics. These findings highlight the important role of behavioral factors in shaping ecological interactions.

Keywords: Predator-prey model, Monod-Haldane, fear effect

Introduction

Ecosystems are shaped by interactions among species, including predator-prey relationships, which play a fundamental role in regulating population dynamics. In ecology, such interactions include predation, competition, mutualism, and parasitism (Ghimire and Wang, 2021). Predator-prey dynamics are influenced not only by population sizes but also by behavior and responses to environmental conditions. One factor that determines the persistence of this interaction is the predator's dependence on prey as a primary food source. In the absence of prey, predator populations will decline and may face extinction over a certain period (Sajidah, 2020).

In nature, predator-prey behavior is also influenced by the fear effect. Prey fear of predators can affect feeding patterns, reproductive behavior, and population distribution, which indirectly influence population dynamics (Sih *et al.*, 2010). Research shows that fear of wolves (Canis lupus) causes ungulate species such as deer (Cervus elaphus) to avoid certain areas to reduce predation risk (Creel *et al.*, 2007). This avoidance reduces feeding time, which impacts the physical condition and reproductive ability of deer. On the other hand, more alert prey behavior also influences predator hunting strategies, demonstrating how fear can affect the overall predator-prey dynamics (Brown *et al.*, 1999). The fear effect also has important implications for ecosystem balance. At the population level, changes in prey behavior due to fear can reduce energy intake, slow population growth, or even increase the risk of mortality due to starvation. Other studies show that the fear effect can alter prey distribution patterns and influence their interactions with other species within the ecosystem (Zanette *et al.*, 2011).

Mathematical ecology plays an important role in understanding predator-prey dynamics, with the Lotka-Volterra model serving as a fundamental framework for describing population fluctuations (Voltera, 1926). A key component of this model is the functional response, which characterizes the relationship between predation rate and prey density. In 1953, Holling introduced three functional response types—Types I, II, and III— describing the relationship between predation rate and prey density (Holling, 1965). Later, Monod and Haldane (1940) developed what is known as the Holling Type IV functional response, which more realistically represents predation rates that change due to predator saturation as prey density increases (Sokol and Howell, 1980). Previous studies have examined predator-prey models using the Monod-Haldane response (Ruan and Xiao, 2001), showing that predator consumption depends on prey density and may lead to predator saturation. Several mathematical models developed in recent years have investigated the influence of fear on system

stability, bifurcation behavior, and population persistence, demonstrating that fear-induced behavioral changes can significantly alter predator–prey dynamics (Chatterjee, 2022; Din et al., 2024; Yang et al., 2025). These studies further emphasize that non-lethal predator effects play a crucial role in shaping ecological interactions and ecosystem stability. However, most existing models consider the fear effect within monotonic functional response frameworks, such as Holling type II or classical Lotka-Volterra models. To the best of our knowledge, limited research has examined predator–prey dynamics by integrating the Monod–Haldane functional response with fear-induced behavioural changes in prey.

Therefore, this study aims to investigate a predator-prey model that combines the Monod-Haldane functional response with the fear effect on prey. A modified Lotka-Volterra model framework with logistic prey growth is developed to capture predator saturation and prey behavioral responses more realistically. The model is analyzed through equilibrium and stability analysis and validated using numerical simulations to explore the effects of fear on predator–prey population dynamics.

Methods

This study adopts a mathematical modeling approach to investigate predator-prey dynamics incorporating the Monod–Haldane functional response and the fear effect on prey. The methodology consists of a literature review, modeling framework, model variables and parameters, model assumptions, analytical methods, and numerical simulations.

Literature Review

The process begins with a comprehensive review of previous research on predator–prey interaction models, functional response formulations, and the incorporation of fear effects in population dynamics. This review provides the theoretical foundation for constructing a biologically meaningful model based on real ecological phenomena.

Modeling Framework

Based on the literature review, a predator–prey model is developed to represent a two-species interaction system. The model incorporates logistic prey growth, the Monod–Haldane functional response to represent predator saturation, and a fear effect term to describe behavioral changes in prey due to predator presence. The detailed mathematical formulation of the model is presented in the Results and Discussion section.

Model Variables and Parameters

Let $x(t)$ and $y(t)$ denote the prey and predator populations at time t, respectively. The parameters used in the model are defined in Table 1.

Table 1. Variables and parameters of the predator-prey model

Symbol	Description
r	Intrinsic growth rate of prey
K	Carrying capacity of prey
β	Maximum predation rate
m	Predator saturation constant
α	Conversion rate of prey biomass into predator biomass
μ	Natural death rate of predator
f	Fear coefficient of prey toward predators

Model Assumptions

The model is constructed under the following general assumptions:

a) The prey population grows logistically in the absence of predators.
b) The predator population depends entirely on prey as a food source.

c) Predation follows a Monod–Haldane functional response, accounting for predator saturation at high prey density.
d) The fear effect reduces prey growth due to predator presence.
e) The environment is homogeneous and spatial movement is not considered.

These assumptions are biologically reasonable and commonly adopted in predator–prey modeling.

Analytical Method

The formulated model is analyzed to determine its equilibrium points and their stability properties. Local stability is examined using Jacobian matrix and eigenvalue analysis. Bifurcation analysis is conducted by varying key parameters to explore qualitative changes in system dynamics. The analytical results are presented and discussed in the Results and Discussion section.

Numerical Simulation

Numerical simulations are performed to verify the analytical results and to illustrate the dynamical behavior of the predator–prey system under different levels of fear intensity. Simulations are carried out using MATLAB, and phase portraits are generated to visualize predator–prey population dynamics. Parameter values are selected based on biological relevance and previous studies.

Results and Discussion

Previous Research

The fear effect refers to the reduction in prey growth rate caused by behavioral changes in response to the presence of predators (Sasmal and Takeuchi, 2020). Research conducted by Zanette, White, Allen, and Michael on song sparrows (*Melospiza melodia*) during breeding periods showed a significant reduction in reproduction not directly caused by predation (Zanette *et al*., 2011). Fear of predators led to a 40% decrease in the number of offspring. This emphasizes that anti-predator responses arising from fear affect population dynamics through behavioral and demographic changes. Wang, Zanette, and Zou proposed a predator-prey model incorporating the fear effect on prey, with the fear effect represented as:

$$F(f, y) = \frac{1}{1+fy}, \qquad (1)$$

The parameter f denotes the prey's fear level toward the predator y.

Kundu et al. (2018) considered a predator-prey model that combines the fear effect as proposed by Wang et al. (2016), while still following the Lotka-Volterra framework. The parameter represents the prey population and represents the predator population. This assumption can be represented in the following system of differential equations:

$$\begin{aligned} \frac{dx}{dt} &= \frac{rx}{1+fy} - dc - bx^2 - cxy, \\ \frac{dy}{dt} &= \alpha xy - \mu y. \end{aligned} \qquad (2)$$

Model (2) shows that fear in prey can affect ecological balance not only through direct predation but also via behavioral changes that impact prey growth rates. Parameters such as represent r, d, b, c, α in order: intrinsic prey growth rate, natural prey death rate, death rate due to competition, predation rate, conversion efficiency of prey biomass to predator biomass, and natural predator death rate. All parameters are assumed to be positive.

Predator-Prey Model with Monod-Haldane Fonctionnel Response

Research by Ruan and Xiao (2021) discusses a predator-prey interaction model with a non-monotonic (Monod-Haldane) functional response, in which predator consumption rate depends on prey population size. The model reflects real-life phenomena such as predator saturation or prey avoidance, whereby predation rate does not necessarily increase as prey numbers rise. The model developed in that study is as follows:

$$\begin{aligned} \frac{dx}{dt} &= rx\left(1-\frac{x}{k}\right)-\frac{xy}{m+x^2}, \\ \frac{dy}{dt} &= \frac{\alpha xy}{m+x^2}-\mu y. \end{aligned} \tag{3}$$

Model (3) assumes all parameters are positive. It exhibits various bifurcation phenomena, including saddle-node, Hopf, and homoclinic bifurcations, depending on parameter values. Parameter r, m, k, α, μ in order: intrinsic prey growth rate, predator saturation level, environmental carrying capacity, conversion rate of prey to predator, and natural death rate of predators.

Model Construction

This study adopts and combines the models developed by Ruan and Xiao with the fear effect model by Wang, Zanette, and Zou. The constructed model considers predator-prey interactions influenced by predator saturation and behavioral changes in prey due to fear. The predator-prey interaction model is built on the assumption that prey population follows logistic growth, as in the modified Lotka-Volterra model, while predators rely on prey as their primary food source. The predation rate follows the Monod-Haldane functional response, which increases with prey population but declines when prey becomes too abundant due to predator saturation.

Based on equations (2) and (3), the following mathematical model incorporating the fear effect and the Monod-Haldane response is developed:

$$\begin{aligned} \frac{dx}{dt} &= \frac{rx}{1+fy}\left(1-\frac{x}{k}\right)-\frac{\beta xy}{m+x^2} \\ \frac{dy}{dt} &= \frac{\alpha\beta xy}{m+x^2}-\mu y \end{aligned} \tag{4}$$

Based on equation (4), $x(t)$ and $y(t)$ represent the population densities of prey and predator, respectively, at time t. The parameter r is the prey growth rate, k is the environmental carrying capacity, f denotes the prey's level of fear toward the predator, β is the predation rate, m represents the predator's saturation effect, α is the conversion efficiency of prey biomass into predator biomass, and μ is the natural death rate of prey. The analytical solution of model (4) yields equilibrium points that can be used to analyze the system's stability and to further understand the population dynamics in the predator-prey interaction.

Equilibrium Points

An equilibrium point $(\boldsymbol{x}^*, \boldsymbol{y}^*)$ is a point that satisfies $\frac{\boldsymbol{dx}^*}{\boldsymbol{dt}} = \mathbf{0}$ dan $\frac{\boldsymbol{dy}^*}{\boldsymbol{dt}} = \mathbf{0}$. The equilibrium points of equation(**4**) can be obtained as follows:

$$x\left(r(x^2+m)-\frac{rx(x^2+m)}{k}-\beta y(1+fy)\right)= \tag{5}$$

$$y\left(\frac{\alpha\beta x}{m+x^2}-\mu\right)=0 \tag{6}$$

Form equations (5) and (6) the following equilibrium points are obtained:
(i) Equilibrium points $E_1 = (0,0)$
(ii) Equilibrium points $E_2 = (k, 0)$
(iii) Interior equilibrium points obtained from the following equations(7) and (8)

$$r(x^2+m)-\frac{rx(x^2+m)}{k}-\beta y(1+fy)=0, \quad (7)$$

$$\frac{\alpha\beta x}{m+x^2}-\mu=0. \quad (8)$$

Thus, solving equations (7) and (8) yields

$$x^* = AX^2+BX+C,$$

$$y^*=\frac{1}{A}\left(\alpha^2\beta r(x^*)-\alpha k\mu r(x^*)-(fkX^2+k\mu X-\alpha m\mu r)\right).$$

where

$$A=\mu, B=-\alpha\beta, C=\alpha\mu$$

Based on the determination of these equilibrium points, four equilibrium points are obtained, namely: $E_1=(0,0), E_2=(k,0), E_3=(x_3^*,y_3^*)$.

1. The equilibrium point $E_1=(0,0)$ represents the extinction of both populations, i.e., the prey and the predator.
2. The equilibrium point $E_2=(k,0)$ represents the extinction of the predator population, while the prey reaches the environmental carrying capacity k.
3. The interior equilibrium points $E_3=(x_3^*,y_3^*)$ and $E_4=(x_4^*,y_4^*)$ represent the coexistence of prey and predator populations.

The local stability analysis of these equilibrium points is carried out by determining the eigenvalues of the Jacobian matrix around each point in order to identify their stability characteristics.

Stability Analysis of Equilibrium Points

The linearization process is applied to the system model (**4**) by determining the eigenvalues of the Jacobian matrix to identify the stability properties of each equilibrium point. The Jacobian matrix derived from the system of equations is as follows:

$$J(x,y)=\begin{bmatrix} \frac{r\left(1-\frac{x}{k}\right)}{1+fy}-\frac{rx}{k(1+fy)}-\frac{\beta y}{x^2+m}-\frac{2\beta x^2y}{x^2+m} & -\frac{r\left(1-\frac{x}{k}\right)f}{(1+fy)^2}-\frac{\beta x}{x^2+m} \\ \frac{\alpha\beta y}{x^2+m}-\frac{2\alpha\beta x^2y}{(x^2+m)^2} & \frac{\alpha\beta x}{x^2+m}-\mu \end{bmatrix}.$$

Stability of the Equilibrium Point $E_1=(0,0)$

Substituting the equilibrium point $\boldsymbol{E_1}$ into the Jacobian matrix from equation (**4**) yields:

$$J_{E_1}=\begin{bmatrix} r & 0 \\ 0 & -\mu \end{bmatrix}$$

The eigenvalues are obtained by solving the characteristic equation $\boldsymbol{det(J_{E_1})-\lambda I)=0}$

$$det(J_{E_1})-\lambda I)=0$$

$$det\left(\begin{bmatrix} r-\lambda & 0 \\ 0 & -\mu-\lambda \end{bmatrix}\right)=0$$

$$(r-\lambda)(-\mu-\lambda)=0$$

$$\lambda_1=r \; or \; \lambda_2=-\mu$$

Assuming all parameters are positive, we have $r>0$ so $\lambda_1>0$ and $-\mu<0$ so $\lambda_2<0$ Therefore, the equilibrium point E_1 is unstable and classified as a *saddle point*.

Stability of the Equilibrium Point $E_2=(k,0)$

Substituting the equilibrium point E_2 into the Jacobian matrix from equation (4) yields:

$$J_{E_2} = \begin{bmatrix} -r & -\dfrac{\beta k}{k^2+m} \\ 0 & \dfrac{2\beta k}{k^2+m} - \mu \end{bmatrix}$$

Next, the eigenvalues are determined by solving the characteristic equation $\boldsymbol{det(J_{E_2}) - \lambda I) = 0}$:

$$det(J_{E_2}) - \lambda I) = 0$$

$$det\left(\begin{bmatrix} -r-\lambda & -\dfrac{\beta k}{k^2+m} \\ 0 & \left(\dfrac{\alpha\beta k}{k^2+m} - \mu\right) - \lambda \end{bmatrix}\right) = 0$$

$$(r-\lambda)\left(\left(\frac{\alpha\beta k}{k^2+m} - \mu\right) - \lambda\right) = 0$$

$$\lambda_1 = -r \; or \; \lambda_2 = \frac{\alpha\beta k}{k^2+m} - \mu$$

Assuming all parameters are positive, we obtain $-r < 0$ so $\lambda_1 < 0$. If $\lambda_2 < 0$ then the equilibrium point E_2 is asymptotically stable and classified as a node, under the condition $\frac{\alpha\beta k}{k^2+m} - \mu < 0$ Conversely, the point becomes unstable if $\frac{\alpha\beta k}{k^2+m} - \mu > 0$.

Stability of the Equilibrium Point $\boldsymbol{E_3 = (x^*, y^*)}$

The linearization of system(4) around the equilibrium point (x^*, y^*) yields the Jacobian matrix:

$$J_{E_3} = \begin{bmatrix} a_{11} & a_{12} \\ a_{21} & a_{22} \end{bmatrix}.$$

where :

$a_{11} = \frac{r\left(1-\frac{x^*}{k}\right)}{1+fy^*} - \frac{rx^*}{k(1+fy^*)} - \frac{\beta y}{x^{*2}+m} - \frac{2\beta x^{*2} y^*}{x^{*2}+m}$

$a_{12} = -\frac{r\left(1-\frac{x^*}{k}\right)f}{(1+fy^*)^2} - \frac{\beta x^*}{x^{*2}+m}$

$a_{21} = \frac{\alpha\beta y^*}{x^{*2}+m} - \frac{2\alpha\beta y^*}{\left(x^{*2}+m\right)^2}$

$a_{22} = \frac{\alpha\beta x^*}{x^{*2}+m} - \mu$

The eigenvalues of the system are obtained by solving the characteristic equation $det(J_{E_3}) - \lambda I) = 0$

$$det(J_{E_3}) - \lambda I) = 0$$

$$det\left(\begin{bmatrix} a_{11}-\lambda & a_{12} \\ a_{21} & a_{22}-\lambda \end{bmatrix}\right) = 0$$

$$(a_{11}-\lambda)(a_{22}-\lambda) - (a_{12}a_{21}) = 0$$

$$\lambda^2 - (a_{11}+a_{22})\lambda + (a_{11}a_{22} - a_{12}a_{21}) = 0$$

The eigenvalues are thus:

$\lambda_1 = \frac{(a_{11}-a_{22}) + \sqrt{(a_{11}-a_{22})^2 - 4(a_{12}-a_{21}) - a_{11}a_{22})}}{2}$

$\lambda_2 = \frac{(a_{11}-a_{22}) - \sqrt{(a_{11}-a_{22})^2 - 4(a_{12}-a_{21}) - a_{11}a_{22})}}{2}$

Assuming all parameters are positive, the stability of E_3 satisfies the following conditions:

Table 2. Stability Conditions for $E_3 = (x^*, y^*)$

Condition	Stability Type
$a_{11} - a_{22} > \sqrt{(-a_{11} + a_{22})^2 - 4(a_{12} - a_{21}) - a_{11}a_{22})}$, $(-a_{11} + a_{22})^2 - 4(a_{12} - a_{21}) - a_{11}a_{22}) > 0$	Unstable node
$a_{11} - a_{22} < \sqrt{(-a_{11} + a_{22})^2 - 4(a_{12} - a_{21}) - a_{11}a_{22})}$, $(-a_{11} + a_{22})^2 - 4(a_{12} - a_{21}) - a_{11}a_{22}) > 0$	Saddle point or stable node
$a_{11} - a_{22} = 0$, $(-a_{11} + a_{22})^2 - 4(a_{12} - a_{21}) - a_{11}a_{22}) > 0$	Saddle point
$a_{11} - a_{22} = 0$, $(-a_{11} + a_{22})^2 - 4(a_{12} - a_{21}) - a_{11}a_{22}) < 0$	Center
$a_{11} - a_{22} > 0$ $(-a_{11} + a_{22})^2 - 4(a_{12} - a_{21}) - a_{11}a_{22}) < 0$	Unstable spiral
$a_{11} - a_{22} < 0$ $(-a_{11} + a_{22})^2 - 4(a_{12} - a_{21}) - a_{11}a_{22}) < 0$	Stable spiral

Numerical Simulation

Numerical simulations are used to ensure consistency between the analytical and numerical results regarding the stability of the equilibrium points and to visualize the system's dynamics. The parameters used in the simulation are obtained from [9] and [12], along with several values determined based on assumptions. Variations in one of the parameters may affect the stability of the equilibrium points, which is visualized through phase portraits using *Pplane*. The parameter values used in the simulation are presented in Table 3 below.

Table 3. Notation of Variables and Parameter Values

Notation	Value	Description
r	8.6	Ruan dan Xiao
K	5.6	Ruan dan Xiao
	0	Wang, Zanette, dan Zou
f	0.6	Assumption
	0.9	Assumption
β	1.9	Ruan dan Xiao
m	2.3	Wang, Zanette, dan Zou
α	1.5	Assumption
μ	0.02	Ruan dan Xiao

The author conducted simulations by modifying the value of the fear effect parameter, as done in previous studies. The purpose of this simulation is to analyze the changes in the stability of each system solution as this parameter varies.

The numerical simulation results are based on the parameter values presented in Table 3, with the fear parameter set to $f = 0$.

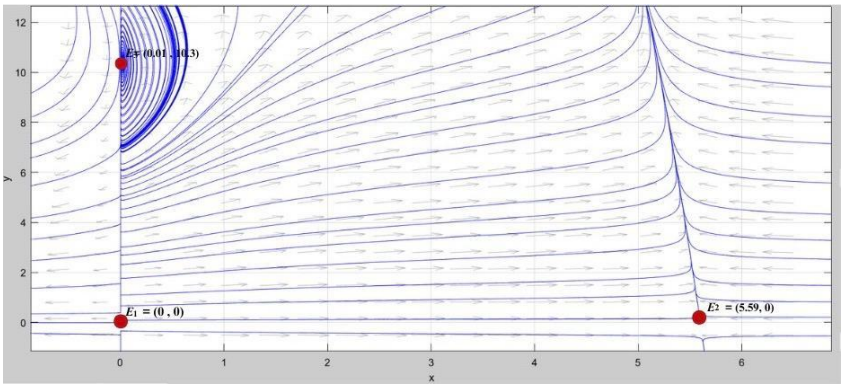

Figure 1. Phase Portrait with $f = 0$

Figure 1 indicates that there is no fear effect on the prey due to the presence of predators. The graph shows direction vectors that represent the dynamic changes in population, along with a red curve that illustrates the system's solution trajectory. At the equilibrium pointE_3 the system exhibits a stable spiral, meaning the prey and predator populations tend to converge toward the equilibrium point $\boldsymbol{E_3}$ in the long term. Since $f = 0$, the prey does not experience a reduction in growth due to fear, so the population dynamics depend solely on direct predator-prey interactions. This results in an oscillatory or spiral pattern toward an equilibrium where both populations can coexist. Based on the parameter values in Table 3 for $f = 0$ the existing equilibrium points are fully presented in Table 4 below.

Table 4. Eigenvalues and Stability at $f = 0$

Equilibrium Point	Eigenvalues	Stability Type
$E_1 = (0,0)$	$\lambda_1 = -0.02$ $\lambda_2 = 8.60$	Unstable Saddle
$E_2 = (5.5999,0)$	$\lambda_1 = -8.60$ $\lambda_2 = 0.454$	Unstable Saddle
$E_3 = (0.0161,10.381)$	$\lambda_1 = -0.01142 + 0.41392i$ $\lambda_2 = -0.01142 - 0.41392i$	Stable Spiral

The numerical simulation results are based on the parameter values in Table 3 with the fear parameter set to $f = 0.6$

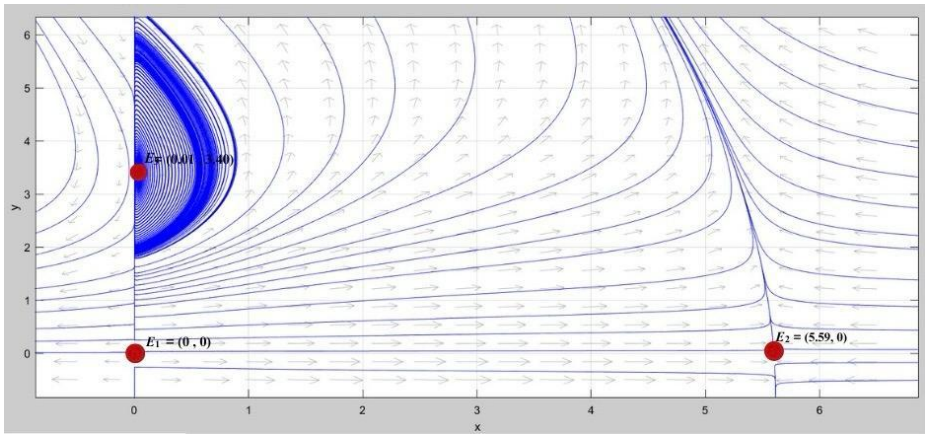

Figure 2. Phase Portrait with $f = 0.6$

In Figure 2, when the parameter value is $f = 0.6$, the fear effect begins to influence the system. As a result, the predator population decreases to 3.41 at the equilibrium point E_3 which is significantly lower than when $f = 0$. In addition, the oscillations that previously occurred begin to diminish, and the system reaches equilibrium more quickly. This indicates that the greater the fear effect, the lower the predator population, and the system tends to become more stable without excessive fluctuations. This suggests that the fear effect helps the prey survive better by reducing direct interactions with predators. The prey becomes more difficult to catch, leading to a decline in the predator population due to decreased food availability. Based on the assumptions for $f = 0.6$ the existing equilibrium points are fully presented in Table 5 below.

Table 5. Eigenvalues and Stability at $f = 0.6$

Equilibrium Point	Eigenvalues	Stability Type
$E_1 = (0,0)$	$\lambda_1 = -0.02$ $\lambda_2 = 8.60$	Unstable Saddle
$E_2 = (5.5999,0)$	$\lambda_1 = -8.60$ $\lambda_2 = 0.454$	Unstable Saddle
$E_3 = (0.0161,3.4089)$	$\lambda_1 = -0.00375 + 0.30676i$ $\lambda_2 = -0.00375 - 0.30676i$	Stable Spiral

The numerical simulation results are based on the parameter values presented in Table 3, with the fear parameter set to $f = 0.9$

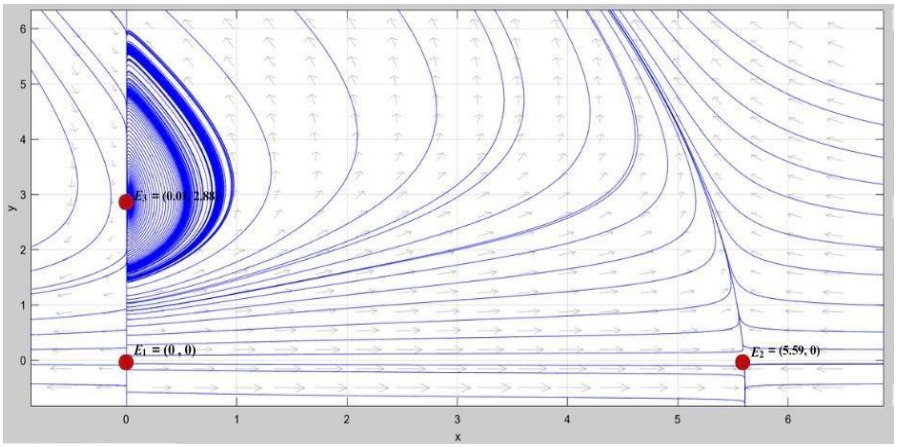

Figure 3. Phase Portrait with $f = 0.9$

The fear effect significantly influences the system. As a result, the predator population decreases drastically to around 2.89 at the interior equilibrium point E_3, which is much lower than when $f = 0.6$. Moreover, the population oscillations that previously occurred begin to disappear, and the system tends to reach equilibrium more quickly. This indicates that the greater the fear effect, the lower the predator population becomes, and the system becomes more stable without excessive fluctuations. In other words, the fear effect helps the prey population survive more effectively by reducing the intensity of direct interactions with predators. As prey become harder to catch, predator populations decline due to the reduced availability of food. Based on the assumptions for $f = 0.9$, the equilibrium points and their stability properties are shown in Table 6.

Table 6. Eigenvalues and Stability at $f = 0.9$

Equilibrium Point	Eigenvalues	Stability Type
$E_1 = (0,0)$	$\lambda_1 = -0.02$ $\lambda_2 = 8.60$	Unstable Saddle
$E_2 = (5.5999,0)$	$\lambda_1 = -8.60$ $\lambda_2 = 0.454$	Unstable Saddle
$E_3 = (0.0161,2.8859)$	$\lambda_1 = -0.00317 + 0.28647i$ $\lambda_2 = -0.00317 - 0.28647i$	Stable Spiral

The simulations show that increasing the fear parameter f significantly affects the system dynamics. At $f = 0$, he system exhibits a stable spiral at point E_3, indicating population oscillations before reaching equilibrium. When $f = 0.6$ the fear effect becomes noticeable, with the stability shifting toward a stable node and the predator population decreasing. At $f = 0.9$, the system becomes more stable and reaches equilibrium faster, with an even lower predator population. The larger the value of f the more the predator population tends to decrease, and the system becomes more stable without oscillations.

Based on the stability analysis, it is known that the stability of the equilibrium point $\boldsymbol{E_2}$ a depends on the value of the parameter $\frac{\alpha\beta k}{k^2+m} - \mu < 0$. Therefore, an experiment is conducted by selecting the value $\beta = 0.05$ which meets this stability condition, to observe the possibility of the equilibrium point E_2 becoming stable under a high fear condition, namely $f = 0.9$.

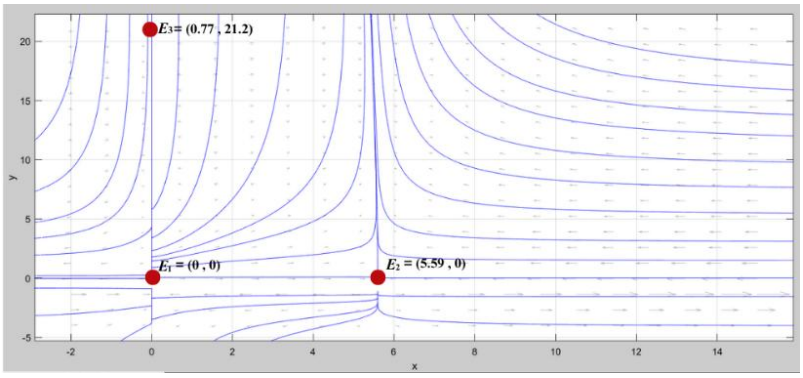

Figure 4. Phase Portrait with$\beta = 0.05$

The simulation results show that the system's solution trajectory moves toward the equilibrium point $E_2 = (5.6\,, 0)$ indicating the dynamics that occur when the fear effect is high and the predation rate is very low. Under this condition, the wolf population is unable to maintain its existence due to limited access to prey and consequently goes extinct. On the other hand, the deer population does not experience significant predation pressure and continues to grow until it reaches the environmental carrying capacity. The high fear level $f = 0.9$ and low predation rate $\beta = 0.05$ cause the system to move toward a state where only the deer population survives. Meanwhile, the interior equilibrium point $E_3 = (0.77\,, 21.2)$ becomes unstable under this condition, as indicated by the trajectory directions around the point moving away from it rather than converging toward it.

Numerical continuation with respect to the parameter β is carried out under the condition of high fear $f = 0.9$ to analyze how changes in the predation rate affect the stability of the system. Starting from $\beta = 0.05$, the point $E_2 = (k\,, 0)$ is asymptotically stable, indicating that the deer population survives while the wolf population goes extinct. The point E_3, although existing, is a stable spiral. As β increases, a Hopf bifurcation occurs at E_3, as shown in Figure 5.

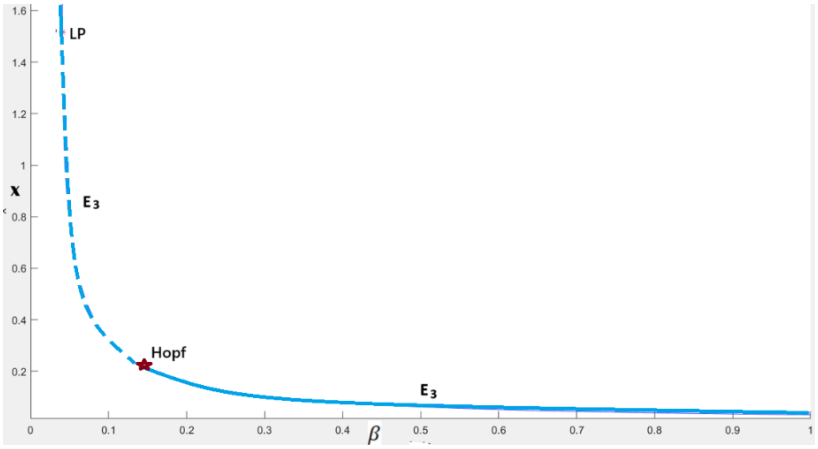

Figure 5. Bifurcation Diagram

Numerical continuation using parameter β reveals the occurrence of a **Hopf bifurcation** at $\beta = 0.055594$ and the emergence of a **Limit Point** indicating a **Saddle-Node bifurcation** at $\beta = 0.040442$ both at the equilibrium point E_3. The Hopf bifurcation occurs at $\beta = 0.055594$ where the previously unstable equilibrium point E_3 becomes stable after crossing the bifurcation threshold. This marks a transition from stability to the emergence of a limit cycle, which represents periodic population fluctuations. At $\beta = 0.040442$, a Saddle-Node bifurcation occurs, in which two equilibrium points disappear, leaving only E_1 and E_2. These results indicate that β significantly influences the system's long-term dynamics—especially when combined with the fear effect. The higher the value of β, the more dominant the predator population tends to become, while a high level of fear suppresses the prey population, resulting in either a new stable state or oscillations, depending on the parameter values.

Biological Interpretation

The results show that the predator–prey system admits three equilibrium points: extinction, prey-only, and coexistence. The coexistence equilibrium represents long-term survival of both populations and exhibits oscillatory dynamics when the fear level is low. As the fear parameter increases, predator population density decreases and population oscillations become weaker, indicating that fear reduces predation success and suppresses predator growth. When the fear level is high and the predation rate is low, the prey-only equilibrium becomes stable, leading to predator extinction. These results demonstrate that fear-induced behavioral changes play a significant role in shaping predator–prey population dynamics and ecosystem stability.

Conclusion

The dynamic analysis reveals the existence of three equilibrium points $E_1 = (0,0)$ represents the extinction of both prey and predator populations, which corresponds to a collapse of the ecosystem where neither species can survive. The equilibrium point $E_2 = (k, 0)$ describes a situation in which the prey population survives at the environmental carrying capacity while the predator population becomes extinct, representing a predator-free ecosystem. The interior equilibrium point E_3 indicates a coexistence state where both populations can persist without extinction. Based on the stability analysis around these equilibrium points, it is found that the point $E_1 = (0,0)$ is unstable of saddle type, while $E_2 = (k, 0)$ is asymptotically stable of node type if the condition $\frac{\alpha\beta k}{k^2+m} - \mu < 0$ and E_3 is a stable coexistence point characterized by a spiral trajectory converging to it, provided certain stability conditions are met.

The numerical simulation results show that the prey's fear parameter significantly affects the system's solution behavior. When there is no fear effect $f = 0$, the prey population tends to go extinct, while the predator population persists. As the fear effect increases to $f = 0.6$ and $f = 0.9$, the prey

population declines more rapidly, and the predator population also decreases due to limited food availability. $\beta = 1.9$, the equilibrium point E_3 which represents the coexistence between deer and wolves, remains a stable spiral for all values of f, indicating that both populations can survive even as fear increases. However, when β is decreased to 0.05 under high fear conditions $f = 0.9$, the equilibrium point E_2 becomes asymptotically stable E_3, becomes unstable. The simulations also reveal the occurrence of bifurcations when the parameter β is varied. Both Hopf and Saddle-Node bifurcations emerge under the condition $f = 0.9$, indicating that small changes in the predation rate can lead to major shifts in ecosystem dynamics. The numerical continuation results show that the Saddle-Node bifurcation occurs at $\beta = 0.040442$ at point E_3 and the Hopf bifurcation occurs at $\beta = 0.055594$.

References

Brown, J.S., Laundré, J.W., and Gurung, M. (1999) The ecology of fear: Optimal foraging, game theory, and trophic interactions, *Journal of Mammalogy*, 80(2): 385–399.

Chatterjee, A. (2022) Modelling the fear effect in prey predator ecosystem incorporating prey patches, *Journal of Computational Analysis and Applications*, 30(1): 114–129

Creel, S., Christianson, D., Liley, S., and Winnie, J.A. (2007) Predation risk affects reproductive physiology and demography of elk, *Science*, 315(5814): 960–960.

Din, D., Naseem, R.A., Shabbir, M.S. (2024) Predator–prey interaction with fear effects: stability, bifurcation and two-parameter analysis incorporating complex and fractal behavior, *Fractal and Fractional*, 8(4):221.

Ghimire, S. and Wang, X.S. (2021) Competition and cooperation on predation: Bifurcation theory of mutualism, *Journal of Biological Systems*, 29(1): 49–73.

Holling, C.S. (1965) The functional response of predators to prey density and its role in mimicry and population regulation, *Memoirs of the Entomological Society of Canada*, 97(S45): 5–60.

Kundu, K., Pal, S., Samanta, S., Sen, A., and Pal, N. (2018), Impact of fear effect in a discrete-time predator-prey system, *Bulletin of the Calcutta Mathematical Society*, 110(3): 245–264.

Ruan, S. and Xiao, D. (2001) Global analysis in a predator–prey system with nonmonotonic functional response, *SIAM Journal on Applied Mathematics*, 61(4): 1445–1472.

Sajidah, F.N. (2020) Analisis kestabilan sistem mangsa-pemangsa tiga spesies dengan fungsi respon Holling tipe II dan fungsi respon Beddington-DeAngelis, *MATHunesa: Jurnal Ilmiah Matematika*, 8(2): 190–194.

Sasmal, S.K. and Takeuchi, Y. (2020) Dynamics of a predator-prey system with fear and group defense, *Journal of Mathematical Analysis*, 481(1): 123–471.

Sih, A., Bolnick, D.I., Luttbeg, B., Orrock, J.L., Peacor, S.D., Pintor, L.M., and Vonesh, J.R. (2010) Predator–prey naïveté, antipredator behavior, and the ecology of predator invasions, *Oikos*, 119(4): 610–621.

Sokol, W. and Howell, J. (1980) Kinetics of phenol oxidation by washed cells, *Biotechnology and Bioengineering*, 23: 2039–2049.

Volterra, V. (1926) Fluctuations in the abundance of a species considered mathematically, *Nature*, 118(2972): 558–560.

Wang, X., Zanette, L., and Zou, X. (2016) Modeling the fear effect in predator–prey interactions, *Journal of Mathematical Biology*, 73: 1179–1204.

Yang, M., Xiang, C., and Yang, Y. (2025) Spatiotemporal patterns in a predator–prey model with anti-predation behavior and fear effect, *Advances in Continuous and Discrete Models*, 20.

Zanette, L.Y., White, A.F., Allen, M.C. dan Michael, C. (2011) Perceived predation risk reduces the number of offspring songbirds produce per year, *Science*, 334: 1398–1401.